Frontiers in Detector Science and Technology

TYPE Review
PUBLISHED 07 February 2025
DOI 10.3389/fdest.2025.1484647

Check for updates

OPEN ACCESS

EDITED BY
Luca Fiorini,
University of Valencia, Spain

REVIEWED BY
Zongde Chen,
Stanford University, United States
Bruce Mellado,
University of the Witwatersrand, South Africa

*CORRESPONDENCE
José Sánchez del Río Sáez,
jose.sanchezdelrio@upm.es

†These authors have contributed equally to this work

RECEIVED 22 August 2024
ACCEPTED 09 January 2025
PUBLISHED 07 February 2025

CITATION
Sánchez del Río Sáez J, Aragonés V, Sánchez Villaluenga T, Davila-Gomez L, Paramio Martínez S, Vázquez-López A, Ballesteros Y, Martínez V, Jiménez JL, Yusuf A, Li X, Ao X, Xiu J and Wang D-Y (2025) Wi-Fi/LoRa communication systems for fire and seismic-risk mitigation and health monitoring. *Front. Detect. Sci. Technol.* 3:1484647. doi: 10.3389/fdest.2025.1484647

Wi-Fi/LoRa communication systems for fire and seismic-risk mitigation and health monitoring

José Sánchez del Río Sáez[1,2,3]*, Víctor Aragonés[1†], Tomás Sánchez Villaluenga[1†], L. Davila-Gomez[1], Sofía Paramio Martínez[1†], Antonio Vázquez-López[2,4], Yolanda Ballesteros[3,4], Vanesa Martínez[2], José Luis Jiménez[2], Abdulmalik Yusuf[2†], Xiaolu Li[2], Xiang Ao[2], Jie Xiu[2] and De-Yi Wang[2]

[1]Universidad Politécnica de Madrid (UPM), E.T.S. de Ingeniería y Diseño Industrial, Madrid, Spain, [2]IMDEA Materials Institute, Madrid, Spain, [3]Mechanical Engineering Department, Universidad Pontificia de Comillas (ICAI), Madrid, Spain, [4]Institute for Research in Technology, Universidad Pontificia Comillas, Madrid, Spain

This article summarizes the work performed by the authors in developing, during the last 2 years, several portable and wireless sensor systems that allowed the analysis of signals collected from multiple sensors based on the Internet of Things (IoT) in emergency contexts. These include fires and earthquakes, situations in which citizens suffer from poor health; participation of individuals in highly physical sports; or cases of materials used in buildings and other structures being subjected to high stress due to natural catastrophes other than the aforementioned fires and earthquakes. Novel material sensors like MXene paper or wallpaper-based ones used as fire detectors and operating remotely via Wi-Fi and LoRa are presented. Furthermore, a Wi-Fi communication system, physically connected to a commercial micro-controller, monitored the temperature and luminosity data. Other devices, such as IoT wireless systems operating under the LoRa protocol in the 868-MHz and 2.4-GHz band region and using RFM95 radio modules as possible risk advisers, are described. For the latter, the sensors integrated were triboelectric energy nanogenerators (TENGs). In addition, TENG smart masks with LoRa emitters were used and played an important role in risk mitigation. As novel systems, an STM32 LoRa board allowed monitoring of the health (heart rate and oxygen saturation) of athletes involved in combat sports, with a nano-IoT Arduino 33 chip being used for monitoring the electrical resistance change in some composite materials. Some of these developments, especially the previously mentioned one, can play an important role in structural health monitoring (SHM) by examining the mechanical properties during service operations in aviation or aerospace fields. A comparison of these systems allowed them to be classified according to the most fitting application.

KEYWORDS

triboelectric sensors, energy generation, seismic sensors, fire retardancy, IoT, LoRa, wireless communications, risk mitigation

10.3389/fdest.2025.1484647

1 Introduction

Natural disasters such as fires or earthquakes, which occur throughout the world, serve as examples of emergency situations that affect several people, especially those who live in the poorest areas of the planet. Various solutions, all based on sensing technology and actuators, such as MEMS (Liu et al., 2022), seismographs (Anderson et al., 2023), geophones (Hou et al., 2021), GPS localizers (Psimoulis et al., 2018) and, among others, accelerometers (Liao et al., 2022), are commonly used to mitigate the possible risks associated with disasters (Freddi et al., 2021). Thus, there are increasingly more examples of institutions working on sensing and predicting threats with novel algorithms and communication platforms (Rahman et al., 2016; Yang et al., 2013; Ekatpure, 2024; Chołda and Jaglarz, 2016; Jia et al., 2023; Krichen et al., 2024).

Populations may suffer from the effects of catastrophes caused either naturally or by people themselves (Blong, 2021), such as pandemics or the lack of resources after damage caused to towns and cities due to abrupt episodes (Williams et al., 2023; Otto and Raju, 2023). In these cases, the combination of various scientific fields (Aven, 2016) that work with electronics and sensing technology (Rak et al., 2021), communication systems (Maleki et al., 2020), materials science (Rezapour et al., 2021; Loa et al., 2024; Cuadros-Rojas et al., 2024), predictive computing and artificial intelligence (Ghaffarian et al., 2023), and novel application developments in medicine by using new materials or creating drugs and medicines for healing are key elements in protecting people around the planet (Tan et al., 2023; Moghayedi et al., 2023; Xu et al., 2023; Tong and Ebi, 2019; Li et al., 2022a).

The works recently published by the authors, all framed in the field of risk mitigation, are examined in this paper. They pursue three general objectives focused on reducing possible risks to the general public and which are mainly caused by either natural or artificial factors. The first one entails lowering the costs of sensors and embedded hardware, software analysis, and visualization programs so that it is easier for the population to access sensitive information (Aziz Al Kabir et al., 2023; Hou et al., 2023). The second one involves producing novel materials that can operate at a low cost and provide highly sensitive sensors (Bahl et al., 2020; Singh and Sehgal, 2022; Li, 2021). The third one involves exploring the capabilities of different communication protocols (Gomes et al., 2016) such as LoRa (LoRa Alliance, 2020) to transmit remotely a low amount of information across long distances (more than 20 km from the emitter in open spaces) and with the aim of increasing the bandwidth to a maximum in the near future. Thus, the use of this protocol in higher frequencies, such as in the novel communication LoRa band of 2.4 GHz, is important in widening data emission and transmission curves. Boards such as the WiMOD Demo board (IMST) with connected temperature radio sensors meet the requirements of high bandwidth and long distance. Such a board is a new application to be developed, which will help in transmitting a greater amount of information across long distances.

Regarding low energy consumption, the literature and the studies already carried out by the authors report that LoRa better meets demands such as systems with communication protocols characterized by a long distance and a low amount of remote information transmission, as reported in (Yusuf et al., 2022; Sánchez del Río et al., 2022; Li et al., 2022b; Li et al., 2023; Vázquez-López et al., 2023; Del Río Sáez et al., 2023). Here, this involves its use as an alarm sensor in situations where there is a sudden increase in temperature or fire ignition in specific locations through the utilization of different material sensors such as MXene or triboelectric energy nanogenerators (TENGs). This shows the relevance that such systems may have in population risk mitigation. Furthermore, the application of warning a population about the risk when strong ground motions shake locations is critical to avoid catastrophes (Rezapour et al., 2021; Leal de Moraes, 2023).

Thus, in order to highlight the relevance that materials and Internet of Things (IoT) have in risk mitigation, we present a brief examination of the materials and instrumentation used in the works. In addition, a deeper description of the integrated electronics and communication systems has been provided for the following: a) a graphene-based Wi-Fi fire alarm, b) a wallpaper-based Wi-Fi fire alarm, c) the sub-GHz LoRa earthquake sensor, d) the thermal fire (TF)-hazard sensor made from TENGs, e) the LoRa fire-retardant IoT smart mask, f) the Heltec Automation LoRa Wi-Fi Kit 32 to monitor patient heartbeat, g) the STM32L072Z-LRWAN warning system to monitor athlete health, h) the Arduino Nano-IoT 33 for structural health monitoring (SHM), and i) the 2.4 Gz LoRa sensor for transmitting higher data rates over long distances. A comparison of the electronic DAQs used in the experiments is performed with the identification of the best application that most closely fits the characteristics. The results obtained with these novel remote sensors are shown and a conclusion proposed.

2 Sensors used for risk mitigation

2.1 A graphene-based Wi-Fi fire alarm

A novel fire alarm is designed by using flame-retardant cellulose paper loaded with graphene oxide (GO) and 2D titanium carbide (Ti_3C_2, MXene) (Li et al., 2022b). A high impact in a risk-mitigation wireless system based on the communication between a Wi-Fi transmitter (XLPCF20) (see Figure 1) and a Wi-Fi receiver (R080A) (see Figure 2) is presented. This system is focused on detecting the increase in the sample temperature under study, which is highly related to an increase in conductivity. As soon as material conductivity reaches a determined value, an electrical circuit designed to supply electrical power to a Wi-Fi transmitter will be active. As a result, the Wi-Fi transmitter will begin to send alarm messages via Wi-Fi as it will have the electrical power needed to operate.

Once the material is calibrated with the proper thresholds, the system may be placed at different locations in closed or open areas where continuous monitoring of environmental parameters is needed, such as the temperature supported by the fire-warning system presented in this work (Li et al., 2022b). As soon as the electrical circuit is closed after electrical resistance transformation of GO, due to a temperature increase or fire, a fire-warning message will be sent to an operator who will be controlling the state of such parameters in another remote location. Moreover, another LCD display could be directly connected to the Wi-Fi emitter in the case a warning message is required at the location where a fire or high temperature increase occurs. In addition, the remote fire-warning

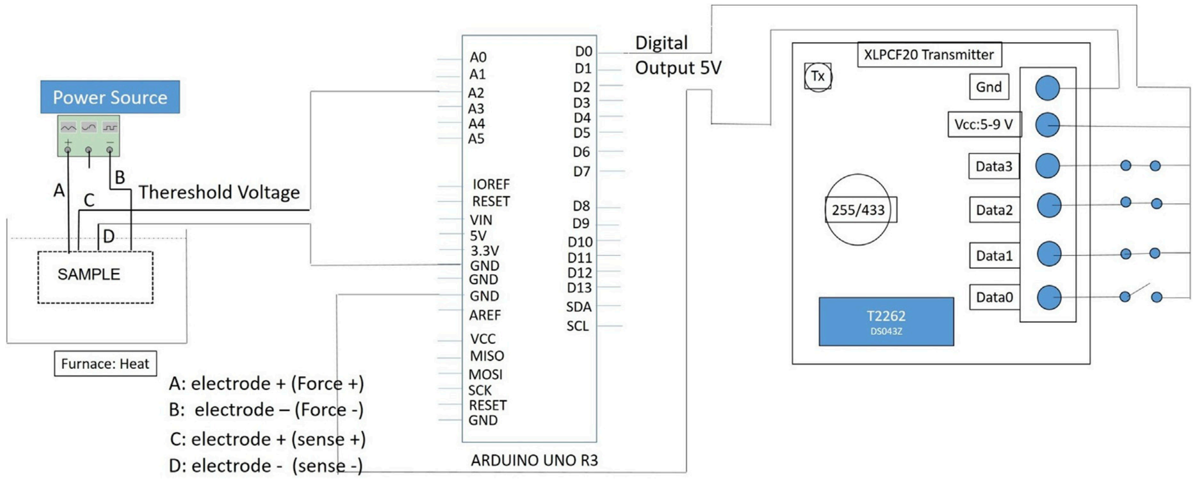

FIGURE 1
Schematics of the warning fire alarm part corresponding to the following: the power source connected to a paper by two force electrodes, the sensing electrodes connected to the Arduino that works as an ADC with a characteristic threshold, and the XLPCF20 Wi-Fi transmitter that will send the Wi-Fi signal to the R08A receptor This figure was published in (Li et al., 2022b) Copyright Elsevier.

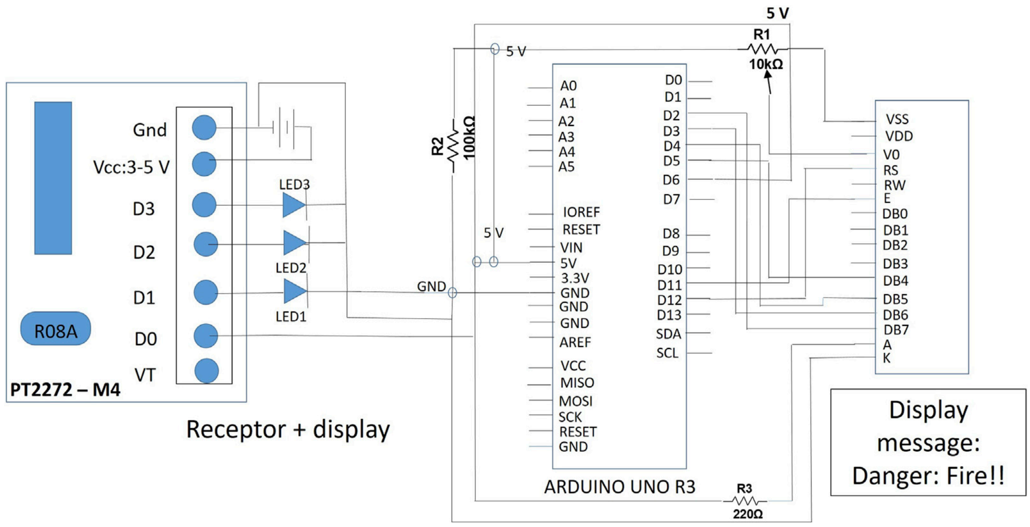

FIGURE 2
Schematics of the warning fire alarm part corresponding to the Wi-Fi receptor unit and the Arduino connected to three LEDs and to an LCD. This receptor unit was programmed with the Liquid Crystal library with the aim of showing a typical alarm message This figure was published in (Li et al., 2022b) Copyright Elsevier.

radius can be extended by using a LoRa IoT system (Figure 3), and automated actuators such as fire extinguishers could be activated once the system warns of the danger.

In this case, the programmable Arduino UNO based on the ATmega328P chip, featuring 1 kb of EEPROM, is used. If a threshold voltage (5 V) is programmed, emitter digital outputs are activated and reach an active state at 5 V. In addition, the XLPCF20 emitter has an antenna with a length of 18 cm, with a maximum transmission distance of 2 km being achieved with a longer one (maximum optimized to 26 cm). In order to avoid interferences in the communication, either for the emitter or for the receptor, 8 bits of coupling were used with three states of codification (high, medium, and low). This emitter has the PT2262 remote control encoder paired with the PT2272 receiver and thus encodes data and address pins into a series-encoded waveform suitable for RF or IR modulation. The voltage operation is 5–9 V, the operating frequency is 315 MHz, the consumption is 50 mW for 9 V in the working mode, and the working current is less than 10 mA (a sensitivity of −105 dBm and a size of 47.5 x 30 x 10 mm). In addition, the PT2272-M4 receiver has a momentary output type, which cannot decode different transmissions. This receiver has a voltage operation of 3–5 V, an

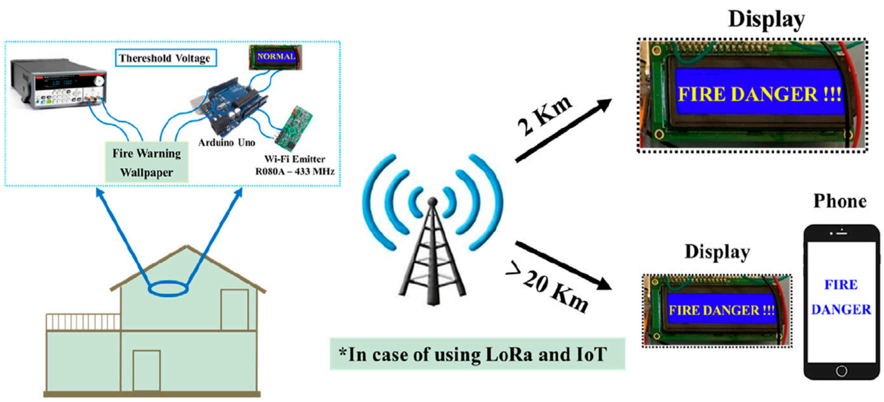

FIGURE 3
Operation flow of the graphene-based Wi-Fi fire alarm with several devices connected to the IoT network This figure was published in (Li et al., 2022b) Copyright Elsevier.

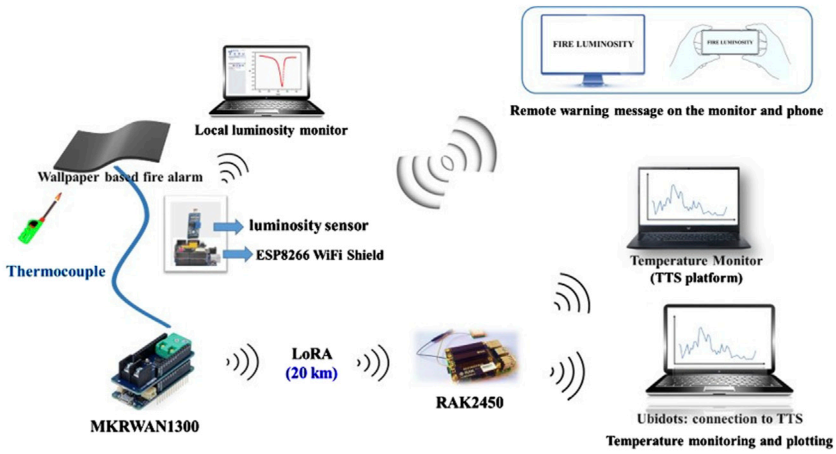

FIGURE 4
Experimental set-up of the temperature and luminosity remote communication system This figure was published in (Li et al., 2023) Copyright Elsevier.

operation frequency of 315 MHz, and a working current of 2.5 mA, and it is of a small size (41x 24x 6 mm). Both the RF emitter and receiver are characterized by low energy consumption.

2.2 A wallpaper-based Wi-Fi fire alarm

A new temperature Wi-Fi sensor, combined with a Wi-Fi luminosity sensor, was employed to monitor the change in temperature and luminosity, both locally and remotely, when a fire was artificially produced to burn a sample. This sample is a wallpaper-based smart fire-warning system based on eco-friendly cellulose paper with a specific flame retardant included (Li et al., 2023).

The OSOYOO ESP8266 Wi-Fi Shield is coupled to an Arduino UNO board to measure luminosity. A photoresistor sensor module is set just below the sample where a fire is produced. Ground-5V and A0 channels from the Arduino were used to supply electrical power to the photoresistor and the electronics system, connected to pins − and + the same as S, respectively. In addition, the integrated development environment (IDE) of Arduino was programmed using WiFiEsp libraries, with the network SSID and password connecting to the Wi-Fi of the facility. Furthermore, a link is generated to enter the web so that luminosity values can be read from any device with internet access. Locally, a PC connected to Arduino and IDE is installed to allow monitoring via the serial port of the luminosity curve measured with the thermoresistance.

Luminosity of the flame was monitored locally using MegunoLink® software and sent through the ESP8266 Wi-Fi board. Both local and remote monitoring processes were running at the same time. The Wi-Fi interface used an HTTP link too, in which luminosity values may be read.

Complementary to the luminosity sensor, a thermocouple is placed close to the paper. This thermocouple is connected to an Arduino MKR Therm shield coupled to a LoRa emitter MKR WAN 1300, which could send the temperature remotely to a RAK2245 Pi Hat concentrator. This concentrator operates as a gateway and receives the packages emitted by the MKR WAN 1300. Furthermore, the RAK is connected to the Wi-Fi, and temperature traces of data are visualized in The Things Stack

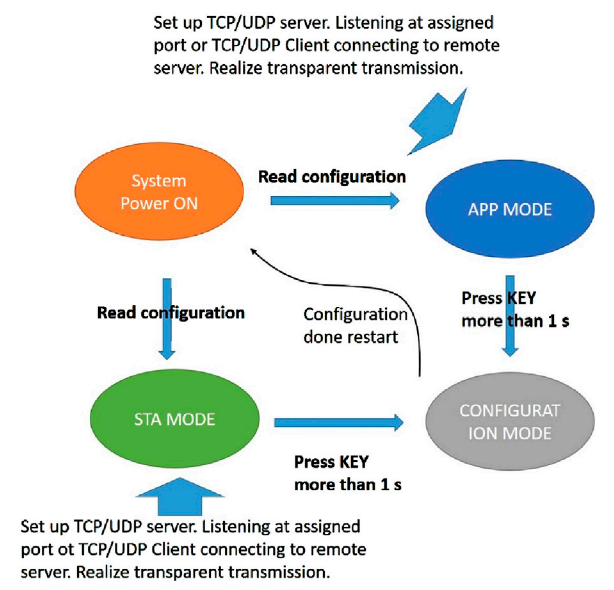

FIGURE 5
ESP8266 work mode relation graph.

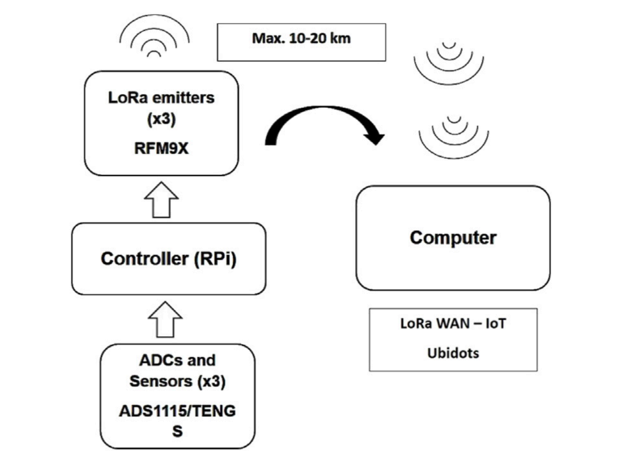

FIGURE 6
Electronics and communications set-up of the 3D axial seismic detector This figure was published in (Del Río Sáez et al., 2023; Li et al., 2022b) Copyright Elsevier.

(TTS) platform. To plot the temperature vs. time, Ubidots IoT software is programmed to be linked to the TTS platform. The temperature measurement can be plotted *in situ* and online (see Figure 4).

This warning communication system, which provides results, will now be examined (Li et al., 2023). First, if a fire occurs, then luminosity values are sent via Wi-Fi to a link that will enable operators working remotely to become aware of the danger. At the same time, the workers can also visualize the luminosity change locally on a computer. Moreover, the thermocouple can detect the temperature change of the wallpaper and send it remotely to a TTN platform. This means that the changed luminosity and temperature can be observed simultaneously with the change, giving full real-time insights into the burning behavior. These two magnitudes measured by the thermocouple and the photoresistor, respectively, will supply information to the operators about the possible danger. If these two parameters reach high values, a fire would possibly occur and that fireproof measures should be implemented. Accordingly, by providing these data of the temperature spectra over time, it offers valuable information on the fire hazard and the subsequent danger, which is essential information for firefighters.

After the temperature increases to 250°C or burning treatment, the warning signal can be monitored within 2 s, indicating the high sensitivity at low temperatures. In addition, it is possible to transmit local and remote messages with the hazard information simultaneously by using a luminosity sensor and temperature sensor. The real-time temperature and luminosity changes can be recorded and transferred to the computer or phone monitors within 20 km.

The OSOYOO ESP8266 Wi-Fi Shield is a UART Wi-Fi one with a low-power-consuming Wi-Fi extension working for Arduino UNO and Mega2560 (there is a 2-bit switch for the function change). Under the Wi-Fi protocol (802.1 b/g/n), the working current when the Wi-Fi is activated is 70 mA, with a maximum current of 200 mA and less than 200 μA operating in the sleep mode. It has a Wi-Fi speed between 110 and 460,800 bits per second (bps) and a serial port bandwidth up to 8 bits. It is lightweight (20 g). As seen in Figure 5, it can operate either in station (STA) or access point (AP) modes. The default mode is AP when the module is configured through the web page.

MKR WAN 1300 has a 32-bit ARM Cortex-M0 SAMD21 of low energy consumption and the Murata CMWX1ZZABZ module that allows the LoRaWAN protocol to be used. The MKRWAN power supply can be two AA or AAA batteries of 3.3 V. A GSM dipole antenna is used to couple LoRa connectivity with the RAK2245 that operates as the gateway in the frequency range of 433/868/915/MHz depending on the country (for Europe 868 MHz). The DC current per I/O pin is 7 mA, and it has seven ADC input pins of 12 bits and one analog input pin of 10 bits. With a length of 67.64 mm and a width of 25 mm, it weighs 32 g. MKR WAN 1300 requires an electrical current of 10 μA in the sleep mode, for which LowPower.deepsleep() library is used. However, when under normal operation, a current of 12 mA was measured.

Connectivity between MKR WAN 1330 and the cloud is performed with the RAK2245 that has a bandwidth of 125 kHz by default. It is the spreading factor (SF) that controls the chip spread spectrum (CSS) and varies from SF1 to SF12. The spreading factors from SF7 to SF12 describe the data package dispersion during the emission and reception time, with it being dependent on the velocity, time of flight, battery duration, and receiver sensitivity. With the choice of SF10, the SF11 and SF12 messages sent are 51 bytes; with SF9, they are 115 bytes; and with SF7 and SF8, they are 242 bytes. The power in the transmission (Tx) band is up to 27 dBm. It has a sensitivity in the reception band of up to −139 dB for the reflection for the bandwidth of 125 kHz in the SF12 configuration.

2.3 The sub-GHz LoRa earthquake sensor

A third system monitors the vibration of a shake table by reproducing a standard impact earthquake in the *Z* direction (Sánchez del Río et al., 2022). For this, the MKR WAN

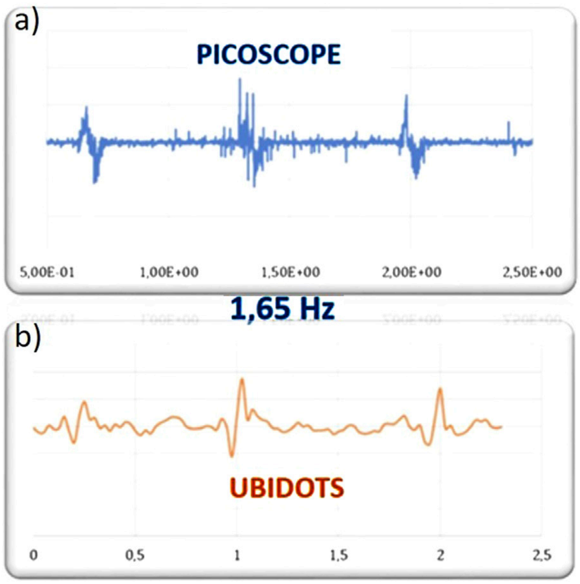

FIGURE 7
1.65 Hz signal monitored in **(A)** the digital oscilloscope PicoScope and **(B)** transmitted via LoRa to the TTN platform and monitored in Ubidots This figure was published in (Yusuf et al., 2022; Li et al., 2022b) Copyright Elsevier (Ubidots).

1300 LoRa transmitter and RAK2245 gateway were utilized to receive the seismic waves and send them to IoT platforms such as Ubidots. The communication frequency plan chosen was EU in the sub-GHz range (868 MHz), and the spreading factor (SF) was 7. For the *X* and *Y* directions, an inertial mass was used as a heavy metallic cylinder. This mass was crabbed into a rectangular cubical box, which was 3D-printed with PLA. TENGs were attached to the beginning and ending parts of the box wall and compressed by the motion of a cylinder producing impacts on the TENGs when the vibration was caused. A 1D vibrating table owned by the Madrid Polytechnic University (UPM-ETSIDI) was used at different frequencies to study the seismic response. Furthermore, in order to monitor them remotely, a novel 3D DAQ system formed by three RFM9X LoRa emitters and ADS1115 of 16-bit voltage sensors were arranged inside another 3D-printed PLA box (Del Río Sáez et al., 2023). Either an RAK2450 or an RAK2245 used as gateways allowed monitoring of the vibrating signals in Ubidots. A schematic of the electronics and communication system is depicted in Figure 6.

Vibration waves with the 3D seismic sensor were detected by means of the three RFM9X LoRa emitters and ADS1115 of 16-bit voltage converters. In order to analyze the maximum rate, the aforementioned TTS LoRa platform was used, and it received data from LoRa transceivers. The 3D-axis LoRa communication device used three TENGs that could continuously and remotely monitor up to 1.65 Hz of frequency vibration signals in Ubidots without losing any package (see Figure 7). These vibration waves were generated with either a traction compression machine or a 3D vibrating table. However, for frequencies higher than 2 Hz, some packages were lost (Del Río Sáez et al., 2023). Furthermore, when only one RFM9X LoRa emitter was used and coupled to the three ADS1115 of 16-bit voltage converters, only one-third of the pulses sent could be received.

The chip RFM9X presents the capability of sending 20 dBm LoRa radio packets, which can easily travel 2 km in the line of sight by using simple wire antennas or up to 20 km with directional antennas and setting tweaks. An SX1276 LoRa®-based module with an SPI interface with +5 to +20 dBm up to 100 mW power output capability is selectable with software. RFM9X has a 100-mA peak during +20 dBm transmit and 30 mA during active radio listening.

Supplementary Table S1 in the supporting information provides a comparison between the MKR WAN 1300 used in Section 2.2, where the wallpaper-based Wi-Fi fire alarm is described, and the RFM95 chip is used in this one, where the sub-GHz LoRa earthquake sensor is studied. This comparison was performed according to the pulse frequency detected, the maximum number of bytes, bit-rate for each package sent, energy consumption, bandwidth used in each case, pulse width measured, and the sample rate. As the RAK2450 limits the rates to the cloud, it is also included for comparison with the others, the same as the ADS1115 16-bit voltage converters.

One of the main aims of configuring the hardware, either for the gateways RFM95 or for the MKR WAN 1300, entails avoiding the loss of packages sent. It is the payload formatter that is responsible not only for decoding the information but also for ensuring the continuity of the signal. For this reason, the timestamp of each of the packages, which is represented by arrays of bytes, is required to be similar to the frequency rate of the data of each package. An example of time lost between packages can be seen in the supporting information, where only 20 ms is lost between packages. An explanation can be found in the supporting information.

2.4 The thermal fire (TF)-hazard sensor made from TENGs

The device (a TF-hazard sensor) presented in this study was designed and developed by the authors and can be found in Yusuf et al. (2022). A TENG made from cellulose paper functionalized with different phytic acid concentrations, via a dip-coating method, with Al layers covering the triboelectric layers and from where Cu electrodes bonded to these Al surfaces connected to electronic devices, was fixed to the base of a hollow metallic cylinder. This fire-retardant TENG is fabricated from flame-retardant materials such as polyimide, which acts as the substrate, Paper@ 50 PA was used as the positive triboelectric layer, and electrospun PVDF-HFP acts as the negative triboelectric layer. The TF-hazard sensor consists of a paraffin rod with a melting temperature in the range of 60oC–69°C and a mass suspended from a spring. As soon as the melting temperature of the phase change material paraffin rod was reached, the load suspended fell and smashed the FR-TENG, generating a V-peak that would operate as a trigger of the subsequent electronic communication system. Different scenarios were planned during the experiment. First, a local advice message was programmed in an Arduino interface so that (when a fire was started or a high temperature was reached) a local advice message could be seen in a display changing from NORMAL to FIRE DANGER. Second, an IoT application was run: an MKR WAN 1300 LoRa board was used as a LoRa emitter, and an RAK2245 Pi Hat concentrator was used as a gateway connected to the Wi-Fi of the facility and operating as a receptor by sending the message programmed in the LoRa emitter to the cloud. In this case, when the

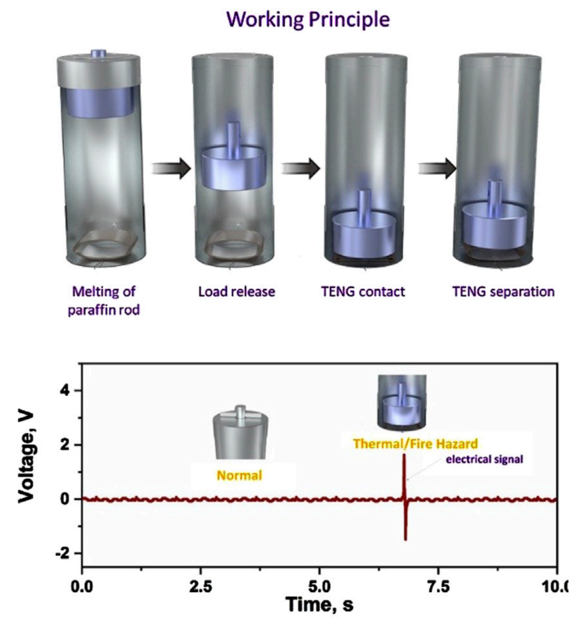

FIGURE 8
Experimental design of the TF-hazard sensor (Copyright Yusuf et al., 2022).

temperature of 60oC–70°C was reached (80°C for the metallic case), the message of FIRE DANGER could be visualized in the TTS platform on any electronic device with access to the internet. Third, an Arduino SIM808 GPS/GRPS/GSM shield connected to an Arduino board was programmed in such a way that as soon as the V peak generated by the TENG was detected, an SMS with the message of FIRE DANGER (or other) would be sent to a smart phone. The photo of the TF-hazard sensor is shown in Figure 8.

All the electronics and communications systems worked properly when the temperature of the paraffin melting point was reached. Local and remote messages could be visualized, respectively, in the Arduino display and TTS platform. Videos that provide supplementary information can be watched in Yusuf et al. (2022), and an example of real operation is presented in Figure 9.

The Arduino SIM808 GPS/GRPS/GSM module is based on the SIMCOM SIM808 chip and offers GPS satellite navigation technology in addition to the functionalities for sending and receiving GSM/GPRS data (that of 2G mobile phones). Due to this module and the use of a SIM card, calls and SMS can be sent and received, being connected to the Internet and determining the coordinates and coordinated universal time (UTC). The main concern of this device is a need to be connected to the satellite network that is the same as the message sending and receiving rate that depends on the saturation of the network (sometimes, this involves a wait of 1 minute when receiving notifications).

2.5 The LoRa fire-retardant IoT smart mask

Another example of a LoRa application, which in this case focuses on the medical and environmental monitoring field, involves the invention of a smart mask designed and developed by Vázquez-López et al. (2023). This mask is made from a fire-retardant TENG and, due to the working principle of the triboelectric effect, breathing of a patient wearing such a mask could be monitored by using the same communication and electronic system as that described in the TG-hazard sensor. In this example, air inhalation/exhalation produces a compression/relaxation of the TENG layers attached to the mask. A V-pulse, due to this mechanical effect on the triboelectric layers, will result in a breathing pulse similar to the one obtained with standard (and more expensive) commercial sensors employed in hospitals. Again, an MKR WAN 1300 board kept in a bracelet and attached to a part of the body such as the forearm and an RAK2245 operating as a gateway to send the alarm message of "BREATHING ANOMALY!!!" to the TTS IoT platform was set as an electronic system. The photograph of the smart mask IoT breathing sensor is provided in Figure 10. Alternatively, a heart-rate-sensor measuring the pulse and the saturation of oxygen in the blood could be integrated into the mask and sent remotely via LoRa. For this, the HELTEC WI-FI LORA V2 ESP32 board was used as a LoRa emitter, the same as a GPS Arduino NEO6M, to locate the patient, and an Arduino ICQANCX was used to detect the cardiac rhythm. This medical information was visualized in Ubidots.

FIGURE 9
Communication system and message interface of the fire-hazard sensor made from TENGs inside the battery of a car (Copyright Yusuf et al., 2022).

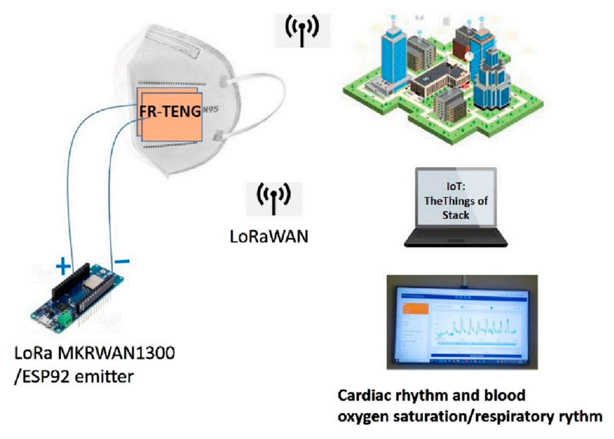

FIGURE 10
Experimental design of the IoT LoRa smart mask This figure was published in (Vázquez-López et al., 2023) Copyright © 2023 American Chemical Society.

Different V-signals generated by the TENGs were monitored in Ubidots using the TTS platform (Vázquez-López et al., 2023). Examples of excited and relaxed states of a patient's breathing could be observed *in situ* by using the LoRa protocol in a smart screen connected to the Internet (see Figure 11).

The potential this sensor has in the medical field is huge as it allows continuous monitoring of the breathing rhythm of patients, the health of citizens who live alone at home, or athletes during training or competition. If there is a parameter that is out of normality, the system will send a message to a central point connected to the Internet, where it will be visualized in any of the IoT platforms such as TTS.

2.6 The Heltec Automation LoRa Wi-Fi Kit 32 to monitor patient heartbeat

This system is designed for monitoring the heartbeat and employs the Heltec Automation LoRa Wi-Fi Kit 32, which is a highly versatile IoT kit that integrates the capabilities of the ESP32 microcontroller with Wi-Fi, Bluetooth, and LoRa connectivity. Due to its compact size, this device is particularly well-suited for patient monitoring, thus providing comfort and freedom of movement. The system incorporates the Adafruit Si7021 temperature and humidity sensor, a compact and lightweight device developed by Silicon Labs, which delivers precise measurements with an accuracy of ±3% relative humidity (within a range of 0%–80% RH) and ±0.4°C for temperature (ranging from −10°C to +85°C). For the purpose of heart-rate monitoring, the HW 827 sensor is utilized, which combines a phototransistor and an LED. This sensor functions by illuminating the skin and detecting variations in the reflected light, corresponding to changes in blood flow, thereby enabling accurate heart-rate measurements that are subsequently displayed in a real-time graphic format. In emergency scenarios, the system is equipped with a buzzer and a button configured in a pull-down position that can be manually activated by either the patient or medical personnel to trigger immediate alerts. Data communication, facilitated through LoRa technology, enables transmission of information over long distances, even in areas with limited network coverage. This ensures comprehensive monitoring capabilities across a hospital and remote locations with restricted access to medical services.

Heartbeat, temperature, and humidity magnitudes of different users could be monitored on the Internet at long distances under the LoRa protocol. In Figure 12A, the main dashboard in Ubidots is shown, displaying the heart rate, temperature, and humidity values measured by the Si7021 sensor, along with the status of the emergency button. The icons and widgets in Ubidots can be customized, allowing users to adjust the interface to their preferences. Additionally, users can view the data more analytically by selecting specific monitored values and zooming in on the desired time periods, as shown in Figure 12B.

The Heltec Automation LoRa Wi-Fi Kit 32 is a kit used in IoT, which is designed and produced by Heltec Automation and based on the ESP32 chip. Furthermore, this device has an OLED screen with Wi-Fi, Bluetooth, and LoRa connection to an Arduino development environment. It has low energy consumption and can be supplied by a 3.7-V lithium battery. When operating via Wi-Fi, it can transmit up to 150 Mbps, and with LoRa, it can transmit 50 kbs. In addition, the maximum transmission power is 19 dB±1 dB, consuming 40 mA (160 mW), and the receiving sensitivity is −135 dBm (40 mA,

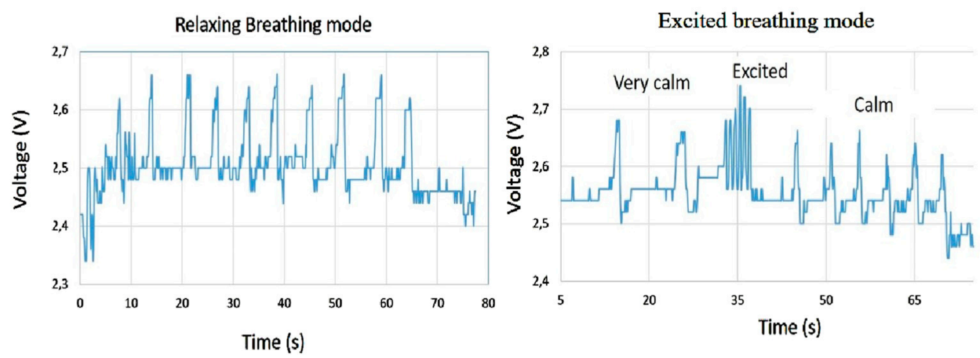

FIGURE 11
Different excitation modes of breathing according to the mask dynamics behavior This figure was published in (Del Bosque et al., 2023) Copyright Elsevier.

FIGURE 12
(A) Heart rate of a patient detected by the Heltec Automation LoRa Wi-Fi module, monitored remotely and visualized in the Ubidots interface. **(B)** The same as in **(A)** but increased to only 1 min long.

meaning 148 mW of power consumption). In deep sleep, a current value of 15 µA is consumed and, as a result, the power of 49.05 µW is consumed. When establishing a LoRa communication between modules or operating as a gateway through the LoRaWAN protocol, often, a 1,200-mAh lithium battery is enough for sending data up to 80,000 times, consuming 120 mA (360 mW) for a 14 dBm data transmission, 140 mA for 17 dBm, and 170 mA for 22 dBm. These values were measured with a Keithley 2400 digital oscilloscope and showed the low energy consumption of LoRa devices, showing high applicability in fields such as sports, health, and environmental measurements.

The Si7021 humidity and temperature detector has a ±3% of humidity precision in the range of 0%–80% and temperature of ±3% in the range of 0°C–80°C. The I2C communication protocol is used for data transfer to the Raspberry or the Heltec Automation LoRa module. Connections are presented in Figure 13. The frequency acquisition rate measured with the Raspberry Pi 0 connected to the RFM95 LoRa emitter and the temperature sensor (Si7021) is 10 Hz in the case of both temperature and humidity being measured and 20 Hz in the case of only one. The HW87 sensor data acquisition rate is 1 Hz.

2.7 The STM32L072Z-LRWAN warning system to monitor athlete health

In this case, a wrist wearable device similar to a smart band built from the STM32L072Z-LRWAN1 microcontroller, together with an oximeter sensor, GNSS, module and algorithms that process the data obtained, was developed. The information provided by the sensor is evaluated to look for patterns to identify situations such as cardiac failure. In addition, emergency signals could be sent manually (see Figure 14).

With this system, if an emergency occurs, the wearable device (Smith et al., 2023) is able to identify it and send an alert signal via the LoRaWAN communication protocol to the central server. This alert contains all the information needed to locate the person wearing the device by means of an identification number and the position obtained by the integrated geolocation module.

In order to avoid possible circumstances where the device runs out of charge, it has an integrated EEPROM memory where the identification information is stored, thus avoiding the need to reload the information into the device.

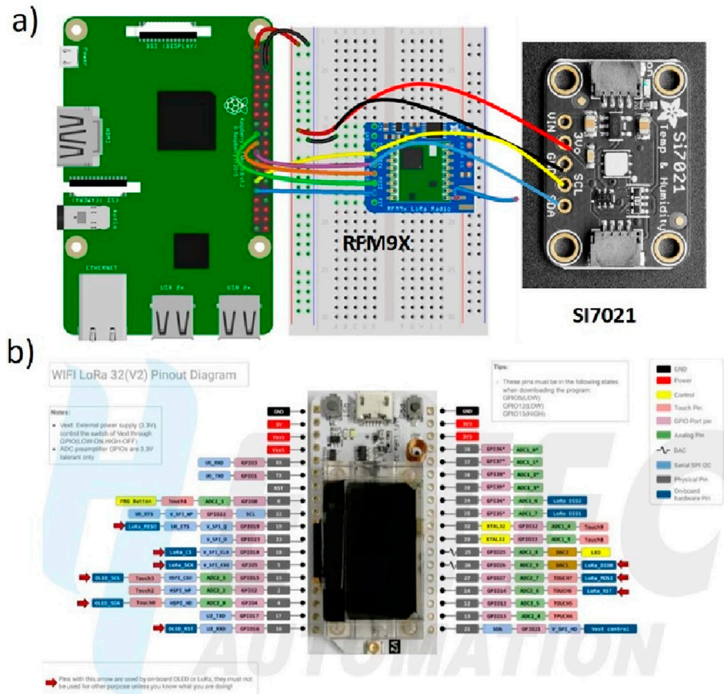

RASPBERRY PI 0	RFM95	SI7021	HELTEC LORA ESP82
3.3 V	Vin	VIN	VIN
GROUND	GND	GND	GND
GPIO5	G0	--	--
GPIO25	RST	--	--
SCK	CLK	SCL	SCL
MISO	MISO	--	--
MOSI	MOSI	--	--
CE1	CS		
SDA	SDA	SDA	SDA

FIGURE 13
(A) Connection between the Raspberry Pi 0, the RFM95, and the temperature sensor Si7021. **(B)** Pinout of the Haltec ESP32 board. **(C)** Table with the pins connected between boards.

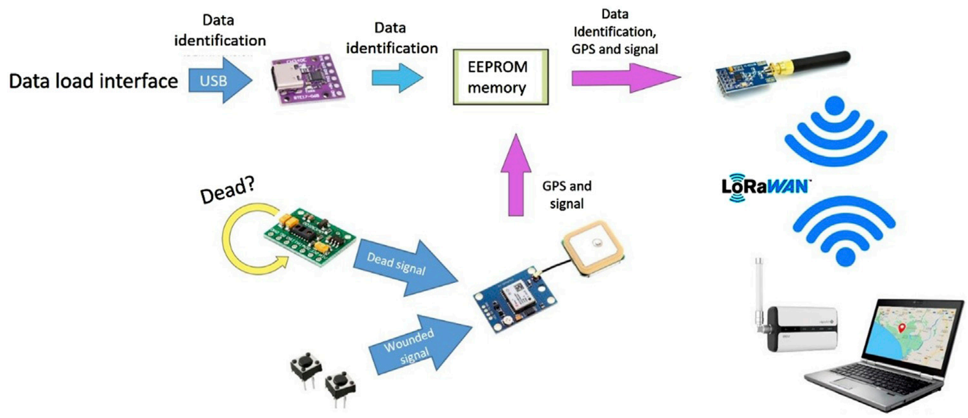

FIGURE 14
Working cycle of the STM32L072Z-LRWAN warning system.

The results obtained with the STM32 board demonstrated the correct operation of the system. Once the identification data were loaded into the device, normal operation was tested by means of terminal debugging. During use, the normal evaluation cycle is initially checked. First, vital signs are obtained; second, evaluation of whether there is an alert or not is carried out; in the event of an emergency, the third step involves searching for the current location of the device by means of the geolocation module and, lastly, sends it by means of the LoRaWAN communication module to the outside.

By simulating an emergency case, the necessary information sent by the device was obtained on the interface of the aforementioned TTS platform. This platform receives the encoded information of the device identification number together with the longitude and latitude where the device is located at the time of the emergency (see Figure 15). Often, depending on the code programmed, this message transmission is repeated three times in a time interval of 5 minutes to ensure the sending and receiving of the data. If the alarm is not reset, the signal transmission is prolonged in time with a longer space between each transmission. It was verified that, once

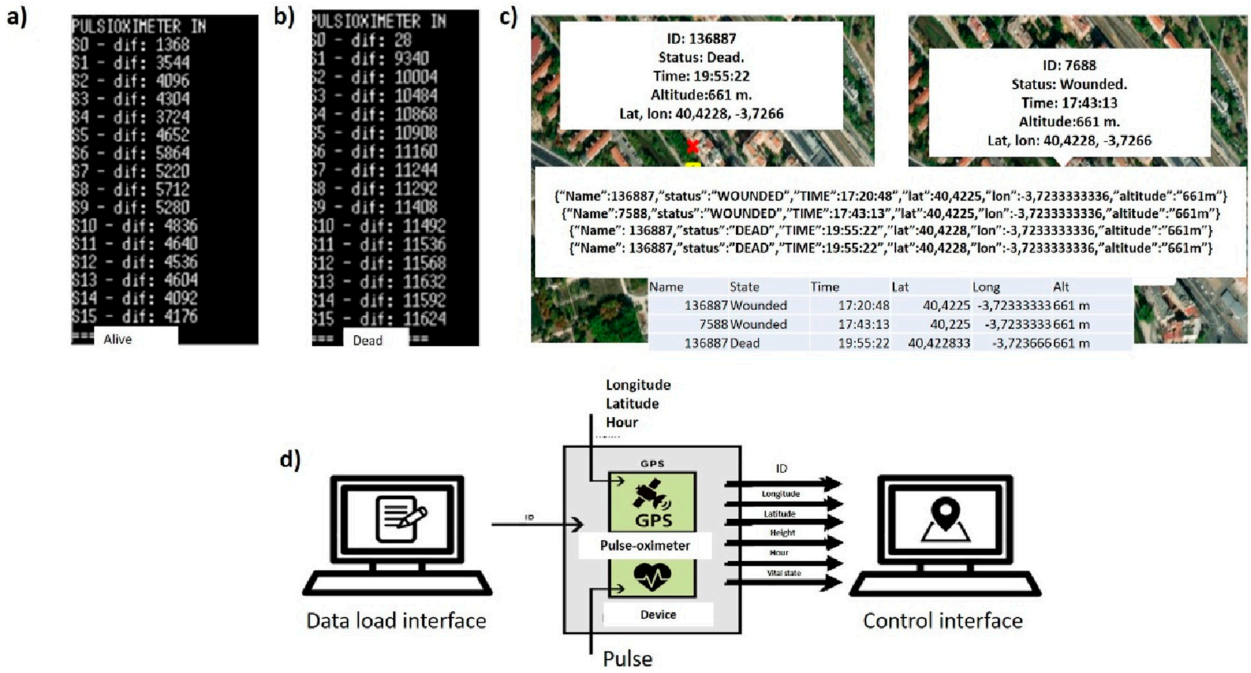

FIGURE 15
(A) Voltage read by the pulse oximeter indicating the heartbeat and the sportsman's state: **(A)** alive or **(B)** in bad conditions; **(C)** geo-localization of the user using the GPS; **(D)** workflow of the data in the microcontroller.

the emergency was reset, the system returned to its normal evaluation cycle.

This system can be employed in the military and surveillance fields in the same manner as in the medical or sports ones. In addition to measuring and monitoring oxygen in the blood and determining if the patient is ill or not, they can be geo-localized by sending the time and spatial coordinates at each moment.

Regarding the electronic design, the development kit STM32L072Z-LRWAN1 can be included in the class of ultralow power devices. This development meets the objectives desired: I2C interfaces, UART, RTC (real-time clock) timer, non-volatile memory EEPROM, and an ability to operate with LoRa technology in a simple way due to the integrated CMWX1ZZABZ-091 module and an SX1276 transceiver with a long-range LoRa mode, which provides an ultra-long-range spread spectrum and high immunity to interference (see Supplementary Figure S6 in the supporting information). The electrical characteristics of this module are provided in Supplementary Table S2, with it being shown that the consumption is 1.95 μA/MHz in the standby mode, 5.5 μA/MHz in the stop mode, and 34 mA/MHz in the transmitter mode.

The main objective of using this device is to detect if the person is alive by monitoring the heartbeat. It also maintained low consumption and adaptability for use as wearable systems as priorities, and the pulse sensor module chosen named MAX30100 is based on the technology implemented by the company Maxim Integrated. It is a sensor that uses the I2C communication protocol and consists of a red-light LED, an infrared light LED, and a phototransistor. The combination of these elements provides values of the amount of both oxygenated and de-oxygenated hemoglobin following the Beer–Lambert law. Together with pulse-beat monitoring, this type of sensor increases its reliability in identifying whether a person is alive or not as it allows further evaluation of the amount of oxygen that passes through the arteries. Additionally, the sensor has a lightweight filter that helps prevent interference and allows temperature measurement. More specific properties are shown in Supplementary Table S3.

The device chosen to geo-localize the user is a module based on the brand NEO-6M-0-001 U-Blox with an UART communication interface. Like any GPS system, it requires a receiving antenna to operate. In this case, a 25-mm square ceramic antenna from the model MOLEX 206640-0001 has been chosen to receive the information packages from the satellite. In addition, the NEO-6M-0-001 receiver module transmits information about the geo-localization via its UART interface by using National Marine Electronics Association (NMEA) messages, from which values of time, longitude, latitude, and altitude are obtained. This module integrates an LED that flashes once per second if the position of the user obtained via GPS is available. Some electronics characteristics of this module are given in Supplementary Table S4.

Information from the data upload interface to the device can be obtained via a USB cable. This cable allows serial communication between the computer and the device. In order to make this information understandable by the device, a converter suitable for this situation is used. In addition, this development kit has a USB port, although it is necessary to solder the plate to use it. The welding of the bridge will allow connecting the lines of the USB connector with the line on which the built-in antenna sends and receives data. As a result, due to the incompatibility between the

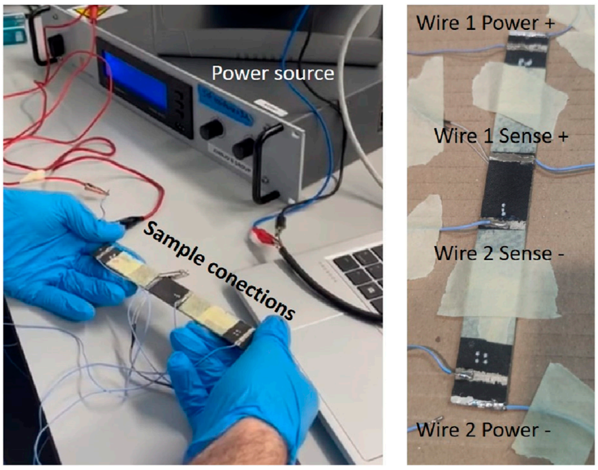

FIGURE 16
Four-wire configuration in the Arduino Nano-IoT 33-based sensor used for structure health monitoring (SHM).

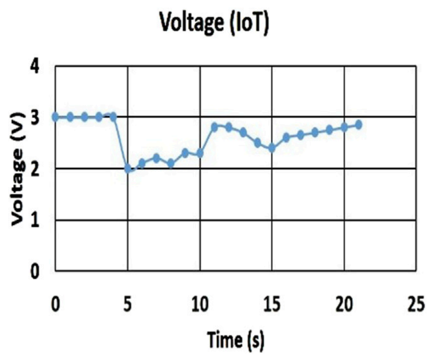

FIGURE 17
Voltage change due to the resistance change of the composite material monitored in the cloud.

necessary configuration and the non-electronic design, the internal use of the board impedes the use of such a port, preventing the use of an external converter that is also necessary. To perform this, a USB-TTL converter was used. The USB input connection part is of type-C, and Tx and Rx pins are the transistor–transistor-logic (TTL) output. The connection map of the STM32L072Z-LRWAN1 development kit is shown in Supplementary Figure S7 of the supporting information and the USB-TTL CH340E in Supplementary Figure S8, with electronic characteristics provided in Supplementary Table S5.

2.8 The Arduino Nano-IoT 33 for structure health monitoring (SHM)

The Arduino Nano-IoT 33 based on the SAMD21 Cortex®-M0+ 32 bit low-power ARM MCU was chosen to remotely monitor the change of voltage existing in a carbon-fiber composite-modified bone probe due to a change in the resistance when bent. For this, the Arduino IoT cloud (Arduino, 2023) was used and configured with a sketch that allowed sending of the voltage measured by two of its analog pins. Although the voltage transmission rate is of 1 Hz, this was enough to monitor the structure of the composite material during service life. The modified composite material consisted of carbon fiber modified with CNT yarns that increased the conductivity and, as a result, a change in the electrical resistance. A high-power electrical source was used to supply voltage (100 V) to the ending parts of the probe (power wires). In addition, two electrodes (sensor wires) were connected to the analog input pins of the Arduino from one end and to two other points of the probe placed between the two power source connections, with the two others in a four-wire configuration, as shown in Figure 16.

The procedure to send information to the cloud is as follows: first, a program in the integrated developments environment (IDE) is used to monitor the voltage and it is sent via Wi-Fi to another Arduino working as a receptor. In addition, in order to send it to the Internet, an IoT cloud of Arduino is activated, and a sketch is programmed to compile the code in the cloud when the electronic board is connected. Some classes such as dashboards are chosen to monitor the physical magnitude to be measured, which, in this case, is voltage. In addition, the subclasses called things present class variables that correspond to the physical magnitudes to measure, and they are associated to a specific device (in this case, the Nano-IoT 33 with its unique ID) and connected to a specific network. As soon as the device is detected and connected, the corresponding dashboard will plot the corresponding data.

The Nano-IoT 33 Arduino board has an energy consumption of 108 mW when collecting and sending data. Furthermore, it works at 3.3 V with a current consumption higher than 33 mA for each of the processes. The frequency acquisition rate in the IoT cloud is in the range of 1.0 Hz–1.2 Hz, and the width band is 0.25 Hz. Frequency signals and waveforms in the IoT cloud are shown in Supplementary Figures S9A–D of the supporting information. In Supplementary Figure S9A, a sinusoidal waveform of 830 mHz is depicted; in Supplementary Figure S9B, a square waveform of 119 mHz is depicted, in Supplementary Figure S9C, a triangular waveform of 257 mHz is depicted; in Supplementary Figure S9D, a square signal of 257 mHz is depicted; in Supplementary Figure S9E, the change in the waveform from square to triangular is depicted; and in Supplementary Figure S9F, the change in the waveform from triangular to sinusoidal is shown. In the last two figures, data loss can be observed because the maximum amplitude is not reached by all the pulses, meaning that the full waveform cannot be detected.

Shifts in the voltage due to resistance change when the composite materials were bent could be measured with the Arduino Nano-IoT 33 and monitored in the cloud in a typical dashboard of the Arduino interface, with it being programmed in the Arduino cloud (see Figure 17). This is important in structural health monitoring (SHM) because it will allow inspection online and *in situ* of the mechanical and structural behavior of composite materials (such as those used in a plane fuselage and vehicle chassis) already manufactured (or during the manufacturing process) and during the service life.

As described before, this invention is highly useful in SHM monitoring because it can be used to assess the structural state of structures, buildings, ports, and aircraft and automotive fuselages where the materials employed sustain mechanical stress and cracks and where defects may appear.

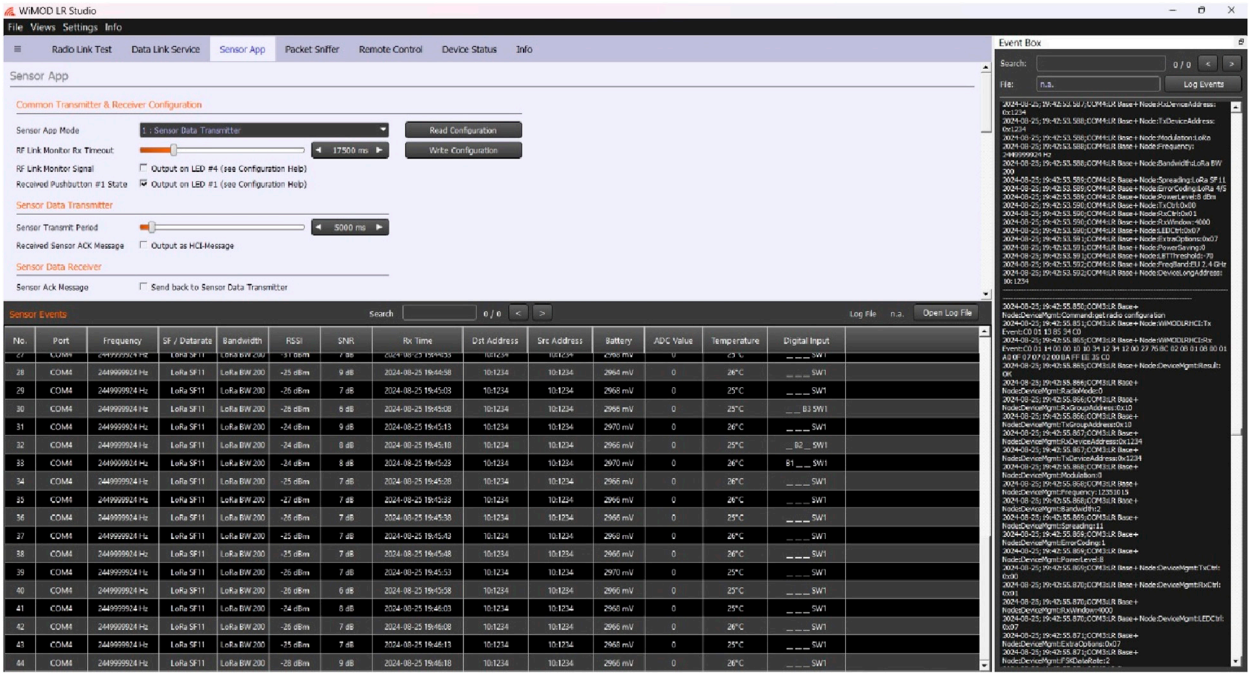

FIGURE 18
WiMOD LR interface, where communication (temperature values) between LoRa modules is shown.

2.9 The 2.4 Gz LoRa sensor

A basic platform (WiMOD demo board) (IMST) for testing different WiMOD radio modules was used to measure the temperature via a two-wire serial interface, with the temperature being transmitted between modules. The USB interface of the demo board allowed communication between the attached radio module and a PC. This demo board uses an Arduino board with LoRa module IM282A. The USB controller (FT232RQ) was turned on once the connection to a PC was established. A gateway 2.4 GHz LoRa will be programmed in the near future to transmit temperature values remotely to IoT LoRa platforms.

Regarding the WiMOD demo board and sensors, the temperature could be transmitted between the emitter and receiver via LoRa. As shown in Figure 18, the temperature between the emitter and receptor was sent by an emitter connected to a receptor, which was in turn connected to the Internet via Ethernet. Other parameters, such as battery power consumption, bandwidth, signal-to-noise ratio (SNR), data rate, and received signal strength indicator (RSSI), could be visualized in the interface. A video of the communication between modules can be seen in SV1 in the supporting information. The classes from the WiMOD and IM282A libraries needed to create an operative interface for sensor communication between modules are shown in Supplementary Figure S10. Here, a serial connection is created, byte interpretation and translation to text is performed, radio communication is established, application control with different windows is carried out, and the service access point (SAP) created. The next steps will entail sending of this magnitude and many others such as humidity, breathing rate, ground oscillations, and alarm messages remotely to the Internet by using the 2.4 GHz LoRa gateway (Chołda and Jaglarz, 2016). As reported previously, the increase in the emission/transmission frequency from 868 MHz to 2.4 GHz (Bluetooth band) will help transmit more information at still very long distances (10 km in inter-urban areas).

3 Comparison of the DAQs

A comparison of the DAQs involved in the setups described above is presented in Table 1, as well as the power consumption either in the sleep or working mode, the bandwidth, the frequency measured between two consecutive LoRa packages, and the applications carried out with them, which can be consulted in the literature.

As reported in Table 1, the DAQ with the least power consumption in the sleep mode is the STM32L072Z-LRWAN1, meaning that it could be used in applications where energy consumption has to be minimized. This could be in situations where there is no possibility either of replacing the batteries or making use of an AC/DC power source. In addition, as on some occasions, it is essential to have the device operating for a long duration; again DAQs with minimum power source consumption are required. This issue is the same in cases where the sensor is operating in the working mode, sending and receiving packages. Here, the higher power spent when the DAQ is receiving or sending packages is chosen. Once again, regarding this specification, the STM32L072Z-LRWAN1 device is the most outstanding DAQ of those studied.

In all the DAQs presented in Table 1, the bandwidth is the same because it is given by the LoRa protocol and the RAK used. This bandwidth is related to the data rate characteristic of the

TABLE 1 Comparison of DAQ power consumption, bandwidth, frequency packages, and data rate of the setups described. Applications carried out with DAQs and found in the literature.

DAQ	Power (sleep/working mode)	Bandwidth	Frequency packages (exp)/ Data rate	Applications
MKR WAN 1300	70 μW/70 mW	125 kHz	0.01 Hz/0.3–27 kbs	Environmental monitoring (Zhao et al., 2024; Zorer et al., 2024; Thoen et al., 2019) smart sensors (Perković et al., 2020; Klaina et al., 2022)
RFM95	3 μW/54–400 mW	125 kHz	0.01 Hz/1.2–20 kbs	Health (Buyukakkaslar et al., 2017), (Jornet-Monteverde et al., 2021), water level (Lukas et al., 2015), and electrical energy (Andre, 2022)
RAK 2245	10 W	125 kHz	0.01 Hz/1.2–20 kbs	Localization (Islam et al., 2024), long communications (Punpigul et al., 2020), and aerial vehicles (Gaggero et al., 2021)
RFM95+ADS1115	3 μW/54–400 mW	125 kHz	1 Hz/0.86 kb	Fire/ground motion (Del Río Sáez et al., 2023)
Heltec (LoRa)	49 μW/360 mW	125 kHz	1 Hz/5.5 kb	Agriculture (Gutierrez et al.; Kodali et al., 2018; Lima Pereira and Cruvinel, 2021), water quality (Sendra et al., 2023), smart sensors (Froiz-Míguez et al., 2020), and LoRa mesh networks (Almeida et al., 2020)
Heltec+Si7021	5 μW/MHz; 180 mW/MHz	125 kHz	1 Hz/5.5 kb	Agriculture (Sokullu, 2022), battery monitoring (Kortbeek et al., 2020), (Al Mamun et al., 2019), etc.
STM32L072Z-LRWAN1	2 μW/1.8 mW	125 kHz	5 Hz/5 kbs	Resource allocation (Garrido-Hidalgo et al., 2023) and environmental (Ali et al., 2019)
STM32+ MAX30100	2.1 μW/1.8 mW	125 kHz	1 Hz, 5 Hz/1 kbs	Medical service robotics (Tian et al., 2019), alcohol detection bracelet (Wu and Li, 2019), and medical care (He et al., 2022; Sheikh et al., 2024; Garcia et al., 2019)
STM32+NEO-6M-0-001 U-Blox	75 μW/36 mW	125 kHz	10 Hz/0.5 kb	Drones recording human activity during pandemics such as COVID (Priyanaka et al., 2022), driving (Konieczka et al., 2023), etc.

DAQ and the sensor, that is, $\frac{2^F}{BW}$, with BW the bandwidth and F the spreading factor previously described. Then, the BW of the DAQ used is determined by the spreading factor chosen for the specific application, with all presenting similar values in the range of 0.3–30 kilobits/s. In addition, after measurement of the time lapse between LoRa packages received by the RAK in the TTS interface, the STM32 board was found to provide the higher rate. This characteristic is important in the choice of the application to work. If higher rates than those offered by the DAQs are needed, then the LoRa protocol would not be the best option.

Many applications may be found in the literature. Most studies are focused on developing LoRa networks with several nodes that upload the information to the cloud in fields such as design of smart sensors, monitoring of environmental parameters in agriculture, measurement of the battery state in automobiles and airplanes, centralization of patient health state in hospitals and residences, and collection of data online from drones with cameras that monitor the activity of infected persons or automation of distinct industry sectors. All of them are immersed in what we call Industry 4.0.

4 Conclusions

With the aim of reducing the impact of catastrophes produced by fires and earthquakes by mitigating risk and monitoring health of citizens suffering from the consequences that abrupt natural and man-made disasters may bring, Wi-Fi and LoRa communication protocols are used in this work with various electronics and communications systems. First, a portable, Wi-Fi, and low-cost wallpaper-based sensor allowed monitoring of temperature and humidity magnitudes. Second, measurement of luminosity and temperature with an MXene-based sensor that increased conductivity with the increase of its temperature and humidity has been examined. Third, a system consisting of an RFM95 LoRa emitter coupled to a Raspberry Pi 400 that could measure changes in the voltage with the ADS1115 voltage converters due to oscillations in the ground in the three directions of the space has been featured. Here, the vibration waves generated were transmitted via LoRa, which could be read in TTS and Ubidots IoT platforms. The fourth, a thermal fire-hazard sensor made of TENGs, has been shown operating inside the battery of a vehicle. In the case of an emergency, such as a fire, a mask will be needed to monitor the health of citizens, monitoring their breathing rhythm, which was developed with a novel IoT textile mask. In addition, the heart rate and temperature of the individual and the humidity of the environment could be measured and sent remotely with the Heltec Automation LoRa module, based on the chip ESP32. Furthermore, vital constants have also been monitored with the STM32L072Z-LRWAN1 module such as the oxygen concentration in blood or the heartbeat of a person using the LoRa protocol. Lastly, temperature data were sent remotely via LoRa with a 2.4 GHz WiMOD demo board between the temperature emitter and receiver LoRa radio-sensors. All the aforementioned devices show significant potential in operating in hazardous environments and have a key role for use in different applications (environmental science, sports activities, and the medical field) with the aim of mitigating environmental risks and decreasing the impact of catastrophes on humans. In addition, a comparison of the DAQs used in the work and presented in this paper according to power consumption, bandwidth, frequency and data rate, and the most common applications used in different fields, has been provided.

Author contributions

JS: conceptualization, data curation, formal analysis, funding acquisition, investigation, methodology, project administration, resources, software, supervision, validation, visualization, writing–original draft, and writing–review and editing. VA: investigation, methodology, software, writing–original draft, and writing–review and editing. TS: investigation, methodology, software, writing–original draft, and writing–review and editing. LD: methodology, supervision, writing–original draft, and writing–review and editing. SP: investigation, writing–original draft, and writing–review and editing. AV-L: formal analysis, investigation, methodology, software, validation, writing–original draft, and writing–review and editing. YB: investigation, methodology, software, writing–original draft, and writing–review and editing. VM: methodology, software, writing–original draft, and writing–review and editing. JJ: methodology, software, writing–original draft, and writing–review and editing. AY: investigation, methodology, software, validation, writing–original draft, and writing–review and editing. XL: formal analysis, investigation, methodology, software, writing–original draft, and writing–review and editing. XA: formal analysis, investigation, methodology, software, writing–original draft, and writing–review and editing. JX: investigation, methodology, software, writing–original draft, and writing–review and editing. D-YW: conceptualization, funding acquisition, investigation, project administration, supervision, writing–original draft, and writing–review and editing.

Funding

The author(s) declare that no financial support was received for the research, authorship, and/or publication of this article.

Acknowledgments

The authors would like to thank IMDEA Materials and, especially, the HPPN group (High-Performance Polymer Nanocomposites group lead by professor De-Yi Wang) for help with using their facilities and new materials with which experiments have been performed over years.

Conflict of interest

The authors declare that the research was conducted in the absence of any commercial or financial relationships that could be construed as a potential conflict of interest.

Publisher's note

Supplementary material

The Supplementary Material for this article can be found online at: https://www.frontiersin.org/articles/10.3389/fdest.2025.1484647/full#supplementary-material

References

Ali, A. I., Partal, S. Z., Kepke, S., and Partal, H. P. (2019). "ZigBee and LoRa based wireless sensors for smart environment and IoT applications," in *Proc. - 2019 IEEE 1st glob. Power, energy commun. Conf. GPECOM*, 19–23. doi:10.1109/GPECOM.2019.8778505

Al Mamun, A., Member, S., Yuce, M. R., and Member, S. (2019). Sensors and systems for wearable environmental monitoring toward IoT-enabled applications: a review. *IEEE Sens. J.* 19 (18), 7771–7788. doi:10.1109/JSEN.2019.2919352

Almeida, N. C., Rolle, R. P., Godoy, E. P., Ferrari, P., and Sisinni, E. (2020). Proposal of a hybrid LoRa mesh/LoRaWAN network. *2020 IEEE Int. Workshop Metrology Industry 4.0 IoT*, 702–707. doi:10.1109/MetroInd4.0IoT48571.2020.9138206

Anderson, J. F., Johnson, J. B., Mikesell, T. D., and Liberty, L. M. (2023). Remotely imaging seismic ground shaking via large-N infrasound beamforming. *Commun. Earth Environ.* 4 (1), 399. doi:10.1038/s43247-023-01058-z

Del Bosque, A., Sánchez–Romate, X. F., Patrizi, D., Del Río Sáez, J. S., Wang, D.-Y., Sánchez, M., et al. (2023). Ultrasensitive flexible strain sensors based on graphene nanoplatelets doped poly(ethylene glycol) diglycidyl ether: mask breathing monitoring for the internet of things, sensors and actuators A: physical 358, 114448.

Andre, H. (2022). "LPWAN communication in IoT network for electrical energy monitoring," in *Proceeding - 2022 int. Symp. Inf. Technol. Digit. Innov. Technol. Innov. Dur. Pandemic*. Padang, Indonesia: ISITDI, 32–35. doi:10.1109/ISITDI55734.2022.9944470

Arduino (2023). Arduino cloud. Available at: https://cloud.arduino.cc/resources/.

Aven, T. (2016). Risk assessment and risk management: review of recent advances on their foundation. *Eur. J. Operational Res.* 253 (1), 1–13. doi:10.1016/j.ejor.2015.12.023

Aziz Al Kabir, M., Elmedany, W., and Sharif, M. S. (2023). Securing IoT devices against emerging security threats: challenges and mitigation techniques. *J. Cyber Secur. Technol.* 7 (4), 199–223. doi:10.1080/23742917.2023.2228053

Bahl, S., Nagar, H., Singh, I., and Sehgal, S. (2020). Smart materials types, properties and applications: a review. *Mater. Today Proc.* 28, 1302–1306. doi:10.1016/j.matpr.2020.04.505

Blong, R. (2021). Four global catastrophic risks – a personal view. *Front. Earth Sci.* 9 (October), 1–17. doi:10.3389/feart.2021.740695

Buyukakkaslar, M. T., Erturk, M. A., Aydin, M. A., and Vollero, L. (2017). LoRaWAN as an e-health communication technology. *2017 IEEE 41st Annu. Comput. Softw. Appl. Conf. (COMPSAC)* 2, 310–313. doi:10.1109/COMPSAC.2017.162

Chołda, P., and Jaglarz, P. (2016). Optimization/simulation-based risk mitigation in resilient green communication networks. *J. Netw. Comput. Appl.* 59, 134–157. doi:10.1016/j.jnca.2015.07.009

Cuadros-Rojas, E., Saloustros, S., Tarque, N., and Pelà, L. (2024). Photogrammetry-aided numerical seismic assessment of historical structures composed of adobe, stone and brick masonry. Application to the San Juan Bautista Church built on the Inca temple of Huaytará, Peru. *Eng. Fail. Anal.* 158 (December 2023), 107984. doi:10.1016/j.engfailanal.2024.107984

Del Río Sáez, J. S., Laguna, A. L., Andolfi, M., Pardo, Á. M., Santos, F., Cascón, R., et al. (2023). LoRA smart sensors for IoT fire and ground motion safety. *2023 6th Experiment@ Int. Conf. (exp.at'23)*, 271–274. doi:10.1109/exp.at2358782.2023.10545832

Ekatpure, R. (2024). Safety protocols and risk mitigation strategies in the implementation of autonomous driving systems. *Adv. Urban Resil. Sustain. City Des.* (February), 1–9.

Freddi, F., Galasso, C., Cremen, G., Dall'Asta, A., Di Sarno, L., Giaralis, A., et al. (2021). Innovations in earthquake risk reduction for resilience: recent advances and challenges. *Int. J. Disaster Risk Reduct.* 60, 102267. doi:10.1016/j.ijdrr.2021.102267

Froiz-Míguez, I., Lopez-Iturri, P., Fraga-Lamas, P., Celaya-Echarri, M., Blanco-Novoa, Ó., Azpilicueta, L., et al. (2020). Design, implementation, and empirical validation of an IoT smart irrigation system for fog computing applications based on Lora and Lorawan sensor nodes. *Sensors Switz.* 20 (23), 1–33. doi:10.3390/s20236865

Gaggero, G. B., Marchese, M., Moheddine, A., and Patrone, F. (2021). A possible smart metering system evolution for rural and remote areas employing unmanned aerial vehicles and internet of things in smart grids. *Sensors* 21 (5), 1–23. doi:10.3390/s21051627

Garcia, C., Trendafilova, I., and Sanchez del Rio, J. (2019). Detection and measurement of impacts in composite structures using a self-powered triboelectric sensor. *Nano Energy* 56, 443–453. doi:10.1016/j.nanoen.2018.11.055

Garrido-Hidalgo, C., Roda-Sanchez, L., Ramírez, F. J., Fernández-Caballero, A., and Olivares, T. (2023). Efficient online resource allocation in large-scale LoRaWAN networks: a multi-agent approach. *Comput. Netw.* 221 (December 2022), 109525. doi:10.1016/j.comnet.2022.109525

Ghaffarian, S., Taghikhah, F. R., and Maier, H. R. (2023). Explainable artificial intelligence in disaster risk management: achievements and prospective futures. *Int. J. Disaster Risk Reduct.* 98 (November), 104123. doi:10.1016/j.ijdrr.2023.104123

Gomes, T., Tapolcai, J., Esposito, C., Hutchison, D., Kuipers, F., Rak, J., et al. (2016). A survey of strategies for communication networks to protect against large-scale natural disasters. *2016 8th Int. Workshop Resilient Netw. Des. Model. (RNDM)* 2011, 11–22. doi:10.1109/RNDM.2016.7608263

Gutierrez, S., Martinez, I., Varona, J., Cardona, M., and Espinosa, R. (2019). "Smart mobile LoRa agriculture system based on internet of things 2019 IEEE 39th cent. Am. Panama conv. CONCAPAN 2019. doi:10.1109/47272.2019.8977109

He, Y., Ren, K., and Shan, S. (2022). "Design of microcontroller-based heart rate and temperature detection system," in *2022 IEEE 5th Int. Conf. Inf. Syst. Comput. Aided Educ.*, 22–25. doi:10.1109/ICISCAE55891.2022.9927650

Hou, X., Li, C., and Fang, Q. (2023). Computer vision-based safety risk computing and visualization on construction sites. *Automation Constr.* 156 (September), 105129. doi:10.1016/j.autcon.2023.105129

Hou, Y., Jiao, R., and Yu, H. (2021). MEMS based geophones and seismometers. *Sensors Actuators A Phys.* 318, 112498. doi:10.1016/j.sna.2020.112498

IMST WiMod shield for Arduino. Available at: https://wireless-solutions.de/products/wsa01-im880b/.

Islam, K. Z., Murray, D., Diepeveen, D., Jones, M. G. K., and Sohel, F. (2024). LoRa localisation using single mobile gateway. *Comput. Commun.* 219, 182–193. doi:10.1016/j.comcom.2024.03.012

Jia, C., Ma, J., Yang, X., and Lv, X. (2023). RAGAN: a Generative Adversarial Network for risk-aware trajectory prediction in multi-ship encounter situations. *Ocean. Eng.* 289 (P1), 116188. doi:10.1016/j.oceaneng.2023.116188

Jornet-Monteverde, J. A., Galiana-Merino, J. J., and Soler-Llorens, J. L. (2021). Design and implementation of a wireless sensor network for seismic monitoring of buildings. *Sensors* 21 (11), 3875. doi:10.3390/s21113875

Klaina, H., Guembe, I. P., Lopez-Iturri, P., Campo-Bescós, M. Á., Azpilicueta, L., Aghzout, O., et al. (2022). Analysis of low power wide area network wireless technologies in smart agriculture for large-scale farm monitoring and tractor communications. *Measurement* 187 (September 2021), 110231. doi:10.1016/j.measurement.2021.110231

Kodali, R. K., Yerroju, S., and Sahu, S. (2018). "Smart farm monitoring using LoRa enabled IoT," in *Proc. 2nd Int. Conf. Green Comput. Internet things, ICGCIoT*, 391–394. doi:10.1109/ICGCIoT.2018.8753086

Konieczka, A., Stachowiak, D., Nski, S. F., and Dworza, M. (2023). Embedded system for learning smooth and energy-efficient tram driving technique. *Energies* 16 (6881), 18. doi:10.3390/en16196881

Kortbeek, V., Bakar, A. B. U., Cruz, S., Yildirim, K. S., Pawełczak, P., and Hester, J. (2020). BFree: enabling battery-free sensor prototyping with Python. *Proc. ACM Interact. Mob. Wearable Ubiquitous Technol.* 4 (4), 1–39. doi:10.1145/3432191

Krichen, M., Abdalzaher, M. S., Elwekeil, M., and Fouda, M. M. (2024). Managing natural disasters: an analysis of technological advancements, opportunities, and challenges. *Internet Things Cyber-Physical Syst.* 4, 99–109. doi:10.1016/j.iotcps.2023.09.002

Leal de Moraes, O. L. (2023). Proposing a metric to evaluate early warning system applicable to hydrometeorological disasters in Brazil. *Int. J. Disaster Risk Reduct.* 87 (November 2022), 103579. doi:10.1016/j.ijdrr.2023.103579

Li, X., Río Saez, J.Sd, Ao, X., Vázquez-López, A., Xu, X., Xu, B., et al. (2022b). Smart Low-temperature responsive fire alarm based on MXene/Graphene oxide film with wireless transmission: remote real-time luminosity detection. *Colloids Surfaces A Physicochem. Eng. Aspects* 651 (June), 129641. doi:10.1016/j.colsurfa.2022.129641

Li, X., Sánchez del Río Sáez, J., Vázquez-López, A., Ao, X., Sánchez Díaz, R., and Wang, D. Y. (2023). Eco-friendly functional cellulose paper as a fire alarming via wireless warning transmission for indoor fireproofing. *Industrial Crops Prod.* 200 (December 2022), 116805. doi:10.1016/j.indcrop.2023.116805

Li, X., Vázquez-López, A., Sánchez del Río Sáez, J., and Wang, D. Y. (2022a). Recent advances on early-stage fire-warning systems: mechanism, performance, and perspective. *Nano-Micro Lett.* 14 (1), 197. doi:10.1007/s40820-022-00938-x

Li, Z. (2021). Recent advances in earthquake monitoring: I – ongoing revolution of seismic instrumentation. *Earthq. Sci.* 34 (0), 177–188. doi:10.29382/eqs-2021-0011

Liao, W., Fei, Y., Ghahari, F., Zhang, W., Chen, P. Y., Kurtulus, A., et al. (2022). Influence of accelerometer type on uncertainties in recorded ground motions and seismic damage assessment. *Bull. Earthq. Eng.* 20 (9), 4419–4439. doi:10.1007/s10518-022-01461-5

Lima Pereira, M. F., and Cruvinel, P. E. (2021). *Development of a LoRa wireless sensor network to estimate agricultural risk*, 35–42.

Liu, H. F., Luo, Z. C., Hu, Z. K., Yang, S. Q., Tu, L. C., Zhou, Z. B., et al. (2022). A review of high-performance MEMS sensors for resource exploration and geophysical applications. *Petroleum Sci.* 19 (6), 2631–2648. doi:10.1016/j.petsci.2022.06.005

Loa, G., Murcia-Delso, J., and Tarque, N. (2024). Efficient beam-based model for reinforced concrete walls considering shear-flexure interaction. *Eng. Struct.* 315 (June), 118365. doi:10.1016/j.engstruct.2024.118365

LoRa Alliance (2020). "*LoRa Alliance*," Available at: https://lora-alliance.org/.

Lukas, L., Tanumihardja, W. A., and Gunawan, E. (2015). "On the application of IoT: monitoring of troughs water level using WSN," in *2015 IEEE Conf. Wirel. Sensors, ICWiSE*, 58–62. doi:10.1109/ICWISE.2015.7380354

Maleki, M., Anvari, E., Hopke, P. K, Noorimotlagh, Z., and Mirzaee, S. A. (2020). Simulation modelling practice and theory. *Psychiatry Res.* 14 (4), 293.

Moghayedi, A., Phiri, C., and Ellmann, A. M. (2023). Improving sustainability of affordable housing using innovative technologies: case study of SIAH-Livable. *Sci. Afr.* 21 (June), e01819. doi:10.1016/j.sciaf.2023.e01819

Otto, F. E. L., and Raju, E. (2023). Harbingers of decades of unnatural disasters. *Commun. Earth Environ.* 4 (1), 280–287. doi:10.1038/s43247-023-00943-x

Perković, T., Šolić, P., Zargariasl, H., Coko, D., and Rodrigues, J. J. (2020). Smart parking sensors: state of the art and performance evaluation. *J. Clean. Prod.* 262, 121181. doi:10.1016/j.jclepro.2020.121181

Priyanaka, P., Ramaraji, R., and Shanmuga, S. K. (2022). Drone based contactless disinfectant spraying system - a safety COVID measures. *Int. J. health Sci.* 6 (June), 3728–3755. doi:10.53730/ijhs.v6nS5.9406

Psimoulis, P. A., Houlié, N., Habboub, M., Michel, C., and Rothacher, M. (2018). Detection of ground motions using high-rate GPS time-series. *Geophys. J. Int.* 214 (2), 1237–1251. doi:10.1093/gji/ggy198

Punpigul, N., Muangkham, M., Anantachaisilp, P., Srisuprapreeda, S., and Singhanat, K. (2020). Long range UAS mission by LPWAN communication. *IOP Conf. Ser. Mater. Sci. Eng.* 965 (1), 012039. doi:10.1088/1757-899X/965/1/012039

Rahman, M. U., Rahman, S., Mansoor, S., Deep, V., and Aashkaar, M. (2016). Implementation of ICT and wireless sensor networks for earthquake alert and disaster management in earthquake prone areas. *Procedia Comput. Sci.* 85 (Cms), 92–99. doi:10.1016/j.procs.2016.05.184

Rak, J., Girão-Silva, R., Gomes, T., Ellinas, G., Kantarci, B., and Tornatore, M. (2021). Disaster resilience of optical networks: state of the art, challenges, and opportunities. *Opt. Switch. Netw.* 42, 100619. doi:10.1016/j.osn.2021.100619

Rezapour, S., Farahani, R. Z., and Morshedlou, N. (2021). Impact of timing in post-warning prepositioning decisions on performance measures of disaster management: a real-life application. *Eur. J. Oper. Res.* 293 (1), 312–335. doi:10.1016/j.ejor.2020.11.051

Sánchez del Río, J., Yusuf, A., Ao, X., Olaizola, I. A., López-Puertas, L. U., Ballesteros, M. Y., et al. (2022). High-resolution TENGS for earthquakes ground motion detection. *Nano Energy* 102 (May), 107666. doi:10.1016/j.nanoen.2022.107666

Sendra, S., Parra, L., Jimenez, J. M., Garcia, L., and Lloret, J. (2023). LoRa-based network for water quality monitoring in coastal areas. *Mob. Netw. Appl.* 28 (1), 65–81. doi:10.1007/s11036-022-01994-8

Sheikh, P. P., Riyad, T., Tushar, B. D., Alam, S. S., Ruddra, I. M., and Shufian, A. (2024). Analysis of patient health using Arduino and monitoring system. *J. Eng. Res. Rep.* 26, 25–33. doi:10.9734/JERR/2024/v26i31090

Singh, T., and Sehgal, S. (2022). Structural health monitoring of composite materials. *Archives Comput. Methods Eng.* 29 (4), 1997–2017. doi:10.1007/s11831-021-09666-8

Smith, A. A., Li, R., and Tse, Z. T. H. (2023). Reshaping healthcare with wearable biosensors. *Sci. Rep.* 13 (1), 1–16. doi:10.1038/s41598-022-26951-z

Sokullu, R. (2022). LoRa based smart agriculture network. *2022 8th Int. Conf. Energy Effic. Agric. Eng. (EE&E)*, 1–4. doi:10.1109/EEAE53789.2022.9831210

Tan, S. Y., Foo, C. D., Verma, M., Hanvoravongchai, P., Cheh, P. L. J., Pholpark, A., et al. (2023). Mitigating the impacts of the COVID-19 pandemic on vulnerable populations: lessons for improving health and social equity. *Soc. Sci. Med.* 328 (April), 116007. doi:10.1016/j.socscimed.2023.116007

Thoen, B., Callebaut, G., Leenders, G., and Wielandt, S. (2019). A deployable LPWAN platform for low-cost and energy-constrained iot applications. *Sensors Switz.* 19 (3), 585. doi:10.3390/s19030585

Tian, S., Yang, W., Grange, J. M. L., Wang, P., Huang, W., and Ye, Z. (2019). Smart healthcare: making medical care more intelligent. *Glob. Health J.* 3 (3), 62–65. doi:10.1016/J.GLOHJ.2019.07.001

Tong, S., and Ebi, K. (2019). Preventing and mitigating health risks of climate change. *Environ. Res.* 174 (April), 9–13. doi:10.1016/j.envres.2019.04.012

Ubidots (2024). Ubidots. Available at: https://es.ubidots.com/.

Vázquez-López, A., del Río Saez, J. S., de la Vega, J., Ao, X., and Wang, D.-Y. (2023). All-fabric triboelectric nanogenerator (AF-TENG) smart face mask: remote long-rate breathing monitoring and apnea alarm. *ACS Sensors* 8 (0), 1684–1692. doi:10.1021/acssensors.2c02825

Williams, B. A., Jones, C. H., Welch, V., and True, J. M. (2023). Outlook of pandemic preparedness in a post-COVID-19 world. *npj Vaccines* 8 (1), 178. doi:10.1038/s41541-023-00773-0

Wu, W., and Li, Z. (2019). *Design of multifunctional bracelet detecting alcohol.* Iaeac, 2342–2345.

Xu, F., Huang, Q., Yue, H., Feng, X., Xu, H., He, C., et al. (2023). The challenge of population aging for mitigating deaths from PM2.5 air pollution in China. *Nat. Commun.* 14 (1), 1–13. doi:10.1038/s41467-023-40908-4

Yang, L., Yang, S. H., and Plotnick, L. (2013). How the internet of things technology enhances emergency response operations. *Technol. Forecast. Soc. Change* 80 (9), 1854–1867. doi:10.1016/j.techfore.2012.07.011

Yusuf, A., Sánchez del Río, J., Ao, X., Olaizola, I. A., and Wang, D. Y. (2022). Potential energy-assisted coupling of phase change materials with triboelectric nanogenerator enabling a thermally triggered, smart, and self-powered IoT thermal and fire hazard sensor: design, fabrication, and applications. *Nano Energy* 103 (July), 107790. doi:10.1016/j.nanoen.2022.107790

Zhao, H., Kam, K. A., Kymissis, I., Mailloux, B. J., and Culligan, P. J. (2024). A LoRaWAN-based environmental sensing network for urban green space monitoring with demonstrated application for stormwater management. *Sustain. Cities Soc.* 115 (September), 105852. doi:10.1016/j.scs.2024.105852

Zorer, R., Mach, E., Centre, I., Mach, V. E., Michele, S., and Tn, A. (2024). A low-cost phenological station as a support tool for viticulture. *BIO Web Conf.* 05003, 2020–2023. doi:10.1051/bioconf/20224405003